Photoluminescence from Electron-Deficient, Mixed-Metal Clusters with $[Pt_2Au]^{3+}$ and $[Pt_2Hg]^{4+}$ Cores

Dawn V. Toronto, Alan L. Balch,* and Dino S. Tinti*

Department of Chemistry, University of California, Davis, California 95616

Received January 11, 1994

There is considerable current interest in the luminescent properties of metal–metal-bonded chromophores.[1] Recently Kunkely and Vogler[2] reported that the triangular cluster **1**, $[Hg_3(dpm)_3](SO_4)_2$,[3] shows intense photoluminescence at 77 K. Bonding within the Hg_3^{4+} unit involves an electron-deficient situation in which the two available valence electrons occupy a three-centered orbital that utilizes contributions from the 6 s orbitals of each mercury. The origin of the luminescence has been ascribed to a trimetal-centered excited state that also involves the three mercury s orbitals. Here we report on related luminescence from analogous electron-deficient, A-frame[4] complexes that are formed by adding d^{10}–s^0 metal centers (Au^IX or $Hg^{II}X_2$) to the Pt–Pt bond of $Pt_2(\mu\text{-dpm})_2X_2$. Representative examples of the products, **2**, $Pt_2(AuX)(\mu\text{-dpm})_2X_2$,[5-7] and **3**, $Pt_2(HgX_2)(\mu\text{-dpm})_2X_2$,[8] have previously been synthesized and characterized by single-crystal X-ray diffraction. These have an electronic configuration that should result in 2-electron, 3-centered bonding within the trinuclear unit.

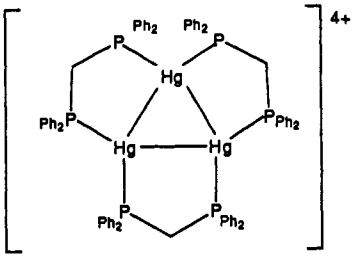

1 **2**

3

Orange dichloromethane solutions of $Pt_2(AuX)(\mu\text{-dpm})_2X_2$ (**2**, X = Cl or Br) show intense red luminescence when frozen at 77 K but no emission at room temperature. Figure 1 shows the absorption (at 298 K) and emission spectra (at 77 K) that were obtained from $Pt_2(AuCl)(\mu\text{-dpm})_2Cl_2$. The absorption spectrum of $Pt_2(AuCl)(\mu\text{-dpm})_2Cl_2$ exhibits three low-energy transitions

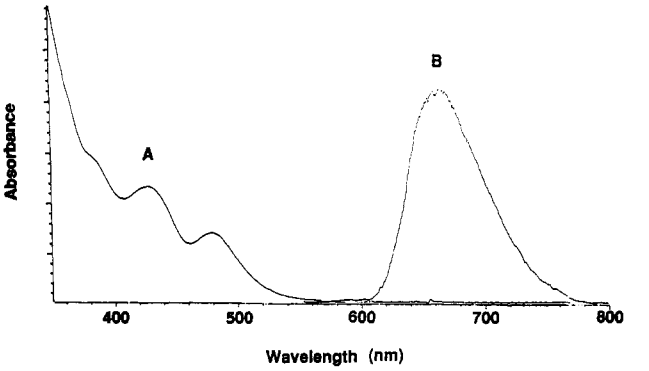

Figure 1. Electronic absorption (A, 298 K) and uncorrected emission (B, 77 K, excitation at 467 nm) spectra from a dichloromethane solution of $Pt_2(AuCl)(\mu\text{-dpm})_2Cl_2$.

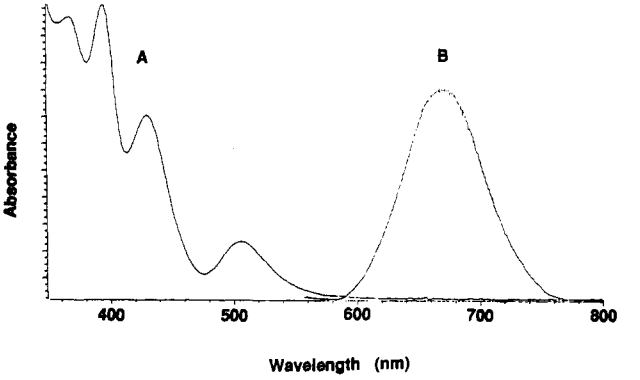

Figure 2. Electronic absorption (A, 298 K) and uncorrected emission (B, 77 K, excitation at 467 nm) spectra from a dichloromethane solution of $Pt_2(HgCl_2)(\mu\text{-dpm})_2Cl_2$.

at λ_{max}/nm (ϵ/M^{-1} cm^{-1}) 394 (3800), 430 (2400), and 506 (810) that show slight shifts to lower energies in the bromo analog, $Pt_2(AuBr)(\mu\text{-dpm})_2Br_2$ (406 (3600), 440 (2300), 516 (800)). These transitions must be metal-centered since the parent complex, $Pt_2(\mu\text{-dpm})_2Cl_2$, shows bands at 362 (2700) and 440 nm (471) (and 368 (3000) and 444 nm (450) for $Pt_2(\mu\text{-dpm})_2Br_2$) which are assigned to the spin-allowed and spin-forbidden $\sigma \rightarrow \sigma^*$ transitions within the Pt–Pt single bond.

The absorption spectra of the mercury(II) halide adducts show similar features with a slight shift to higher energy: $Pt_2(HgCl_2)(\mu\text{-dpm})_2Cl_2$, 382 (2300), 428 (2100), 480 nm (1500); $Pt_2(HgBr_2)(\mu\text{-dpm})_2Br_2$, 398 (3500), 428 (2400), 486 nm (1900). Figure 2 shows the absorption and emission spectra for $Pt_2(HgCl_2)(\mu\text{-dpm})_2Cl_2$. For both the gold and mercury clusters a single low-energy emission is observed: $Pt_2(AuCl)(\mu\text{-dpm})_2Cl_2$, 674 nm; $Pt_2(AuBr)(\mu\text{-dpm})_2Br_2$, 660 nm; $Pt_2(HgCl_2)(\mu\text{-dpm})_2Cl_2$, 677 nm; $Pt_2(HgBr_2)(\mu\text{-dpm})_2Br_2$, 660 nm. The excitation profiles for these emissions parallel the absorption spectra in all cases. $Pt_2(\mu\text{-dpm})_2Cl_2$ or $Pt_2(\mu\text{-dpm})_2Br_2$ themselves show very weak luminescence at 627 nm. Unlike the case with **1**, **2** and **3** are stable to light and prolonged photolysis does not result in extrusion of the added group (AuX or HgX_2) from the trinuclear unit.

In order to probe the binding within the clusters, standard SCF–Xα–SW calculations[9-11] were performed on $Pt_2(PH_3)_4Cl_2$ in both a D_{2h} and a C_{2v} geometry and on $Pt_2(AuCl)(PH_3)_4Cl_2$ and

(1) Balch, A. L. In *Metal-Metal Bonds and Clusters in Chemistry and Catalysis*; Fackler, J. P., Jr., Ed.; Plenum Press: New York, 1990; p 299. Roundhill, D. M.; Gray, H. B.; Che, C.-M. *Accounts Chem. Res.* **1989**, *22*, 55. Zipp, A. P. *Coord. Chem. Rev.* **1988**, *84*, 47. Wang, S.; Fackler, J. P., Jr.; King, C.; Wang, J. C. *J. Am. Chem. Soc.* **1988**, *110*, 3308. Weissbart, B.; Balch, A. L.; Tinti, D. S. *Inorg. Chem.* **1993**, *32*, 2096.
(2) Kunkely, H.; Vogler, A. *Chem. Phys. Lett.* **1993**, *206*, 467.
(3) Hämmerle, B.; Müller, E. P.; Wilkinson, D. L.; Müller, G.; Peringer, P. *J. Chem. Soc., Chem. Commun.* **1989**, 1527.
(4) Hoffman, D. M.; Hoffmann, R. *Inorg. Chem.* **1981**, *20*, 3543.
(5) Arsenault, G. J.; Manojlović-Muir, Lj.; Muir, K. W.; Puddephatt, R. J.; Treurnicht, I. *Angew. Chem., Int. Ed. Engl.* **1987**, *26*, 86.
(6) Manojlović-Muir, Lj.; Muir, K. W.; Treurnicht, I.; Puddephatt, R. J. *Inorg. Chem.* **1987**, *26*, 2418.
(7) Arsenault, G. J.; Puddephatt, R. J. *Can. J. Chem.* **1989**, *67*, 1800.
(8) Sharp, P. R. *Inorg. Chem.* **1986**, *25*, 4185.

0020-1669/94/1333-2507$04.50/0

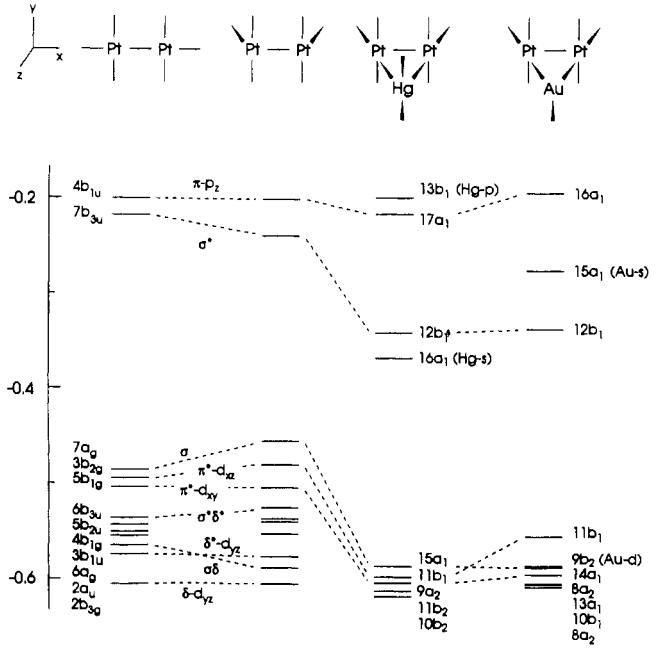

Figure 3. Orbital energies in rydbergs from SCF–Xα–SW calculations for $Pt_2(PH_3)_4Cl_2$ and the mixed-metal clusters.

$Pt_2(HgCl_2)(PH_3)_4Cl_2$ in C_{2v} geometries. The C_{2v} geometries for the first two complexes used Cl–Pt–Pt bond angles of 150°. In the third complex, the Cl–Pt–Pt angle was 160° and the geometry about the mercury was a flattened tetrahedron. The PH_3 moieties were oriented so that there were four close H···H contacts that were parallel to that Pt–Pt bond (x) direction. The remaining angles and the bond distances were taken from X-ray crystallographic data on representative complexes.[5-8]

The calculated energies of the higher valence orbitals, which are numbered with neglect of the core levels, are summarized in Figure 3. The major change engendered in $Pt_2(PH_3)_4Cl_2$ with bending of the Cl–Pt–Pt angle from 180 to 150° is a reduction in the LUMO–HOMO gap by 0.052 Ry (1 Ry = 13.6 eV). Upon bending of this Cl–Pt–Pt angle, the energy of the HOMO, $7a_g$ ($10a_1$), which is largely Pt–Pt dσ, increases and the energy of the LUMO, $7b_{3u}$ ($10b_1$), which is largely Pt–Pt dσ*, decreases. This is the anticipated result for a reduction in the Pt–Pt dσ-overlap that accompanies bending. The more tightly bound orbitals also show changes, but only one clear reversal occurs in the energy ordering of the orbitals that have large Pt-d character (δ*-d_{yz} and $\sigma\delta$). The foregoing results are in good agreement with the calculations of Hoffman and Hoffmann,[2] although some small differences occur in the relative energies of the deeper orbitals.

Adding the third metal center leads to a stabilization of both the LUMO (σ*, b_1) and HOMO (σ, a_1) from the bent parent. These orbitals also acquire character of the added metal. The σ orbital is more affected. Its Pt character, based on the partitioned charges, drops from 56% to 26% in the Pt_2Hg cluster and to 32% in the Pt_2Au cluster, while the added metal contributes 11% and 17%, respectively. The Hg character is mainly p_z with smaller amounts of s (2%) and d (3%), while the Au character is largely s (10%) and p_z (7%) with negligible d contribution. The remaining character is associated mainly with the chloride ligands. Similar, but much smaller, changes occur in the σ* orbital. Its platinum character drops from 52% to 48% in both clusters, with the added metal contributing 5% and 7%, respectively. In terms of the predictions of Hoffman and Hoffmann,[4] the bonding in the clusters is dominated by the a_1 interaction, with the b_1 interaction much less effective. Sharp[8] reached the same conclusion in **3** from a consideration of ^{31}P NMR and structural data.

Differences in the two clusters result from the lower energy of the orbitals on mercury than on gold. For example, in the clusters, the π*-d_{xz} (b_1) orbital of the parent gains Au-d (16%) and Cl-(Au)-p (20%) character, whereas it does not gain any Hg or Cl(Hg) character. The combined effects lead to differences in the composition of HOMOs and LUMOs of the two clusters. In the Pt_2Hg cluster, the HOMO ($15a_1$) remains the σ orbital, but the LUMO ($16a_1$) is largely Hg-s with the σ* ($12b_1$) slightly higher in energy. The π*-d_{xz} ($11b_1$) becomes the HOMO in the Pt_2Au cluster with the LUMO remaining σ* ($12b_1$). The LUMO–HOMO gap, however, is surprisingly constant among the bent parent (2.92 eV) and the two clusters (2.96 eV). The lowest energy excitation also has the same A_1 symmetry in the two clusters.

The expected spectral consequences of the preceding are that the absorption spectra of the two adducts would show a red shift from the undistorted parent and differ in detail but that the energy of the lowest excited states in the two adducts would be similar. The experimental results agree with these predictions. The absorption spectra of the adducts are red shifted from the parent complex. On the basis of the lowest energy peaks in the absorption spectra, the observed shifts are 0.2–0.4 eV in the adducts, compared with an expected shift of 0.5 eV based on the calculated LUMO–HOMO gaps. Figures 1 and 2 also show that the absorption spectra of the two adducts are different in their details. However, the energies of their lowest excited states, as indicated by the onsets of the absorption spectra or peaks of the emissions, are very similar. The mean of the lowest energy absorption and emission peaks in the adducts yields ≈2.2 eV, whereas the calculations predict 2.9 eV for the lowest energy excitation. The energy comparisons are, of course, only semiquantitative since state energies were not calculated.

Acknowledgment. We thank the National Science Foundation (Grant CHE 9022909) for support, Johnson Matthey, Inc., for a loan of precious metal salts, and Bruce Noll for some early observations.

(9) The program, written by M. Cook and D. A. Case, was obtained from QCPE and implemented on a MicroVAX 3100. The angular bases used l_{max} equal to 4 for the outer shell, 3 for the metals, 2 for P and Cl, and 0 for H. The exchange parameters were taken from Schwarz,[10] with valence-electron-weighted averages used in the interatomic and outer regions. Sphere radii were chosen by the "nonempirical" Norman criterion.[11] The quasirelativistic option was used for the metal. All core levels were treated as single atom functions.

(10) Schwarz, K. *Phys. Rev. B* **1972**, *5*, 2466.
(11) Norman, J. G. *Mol. Phys.* **1976**, *31*, 1191.